Cellulose (2014) 21:2665–2678
DOI 10.1007/s10570-014-0269-4

ORIGINAL PAPER

All-cellulose nanocomposite fibers produced by melt spinning cellulose acetate butyrate and cellulose nanocrystals

Saleh Hooshmand · Yvonne Aitomäki · Mikael Skrifvars · Aji P. Mathew · Kristiina Oksman

Received: 9 February 2014 / Accepted: 18 April 2014 / Published online: 10 May 2014

Abstract Bio-based continuous fibers were prepared by melt spinning cellulose acetate butyrate (CAB), cellulose nanocrystals (CNC) and triethyl citrate. A CNC organo-gel dispersion technique was used and the prepared materials (2 and 10 wt% CNC) were melt spun using a twin-screw micro-compounder and drawn to a ratio of 1.5. The microscopy studies showed that the addition of CNC in CAB resulted in defect-free and smooth fiber surfaces. An addition of 10 wt% CNC enhanced the storage modulus and increased the tensile strength and Young's modulus. Fiber drawing improved the mechanical properties further. In addition, a micromechanical model of the composite material was used to estimate the stiffness and showed that theoretical values were exceeded for the lower concentration of CNC but not reached for the higher concentration. In conclusion, this dispersion technique combined with melt spinning can be used to produce all-cellulose nanocomposites fibers and that both the increase in CNC volume fraction and the fiber drawing increased the mechanical performance.

S. Hooshmand · Y. Aitomäki · A. P. Mathew · K. Oksman (✉)
Division of Materials Science, Composite Centre Sweden, Luleå University of Technology, Luleå, Sweden
e-mail: kristiina.oksman@ltu.se

M. Skrifvars
School of Engineering, University of Borås, Borås, Sweden

Keywords Cellulose nanocrystal · Reinforcement · Melt-spinning · Fibers · Mechanical properties

Introduction

Melt spinning is one of the most economical and convenient methods for manufacturing continuous man-made fibers in large quantities for the textile industry. From the time when the first man-made fiber, based on Nylon 6.6, was synthesized by melt spinning, the fiber industry has continuously been developing and different techniques have been applied to improve the processability and properties of the spun fibers (O'Brien and Aneja 1999). One way to improve the mechanical properties of a polymer is to add a second phase as reinforcement. However in fiber manufacturing, since the diameter of the fiber is small, the use of traditional reinforcing elements are not possible due to their large size. Therefore, nanosized reinforcements, defined as materials in which at least one dimension is less than 100 nm (Schadler 2004), can potentially be an effective way to improve the mechanical properties and overcome the size factor. Carbon nanotubes (CNT) (Haggenmueller et al. 2000; Pötschke et al. 2005; Fornes et al. 2006; Mazinani et al. 2010; Pötschke et al. 2010; Hooshmand et al. 2011; Scaffaro et al. 2012), layered-silicates (Yoon et al. 2004; Solarski et al. 2008; Lee and Youn 2008) and cellulose nanocrystals (CNC) (John et al. 2013;

Hooshmand et al. 2014) are examples of the nanosized reinforcements which have been combined with different polymers with the goal to develop melt spun fibers with new functionalities and improved mechanical properties. These additives can improve electrical conductivity (Haggenmueller et al. 2000; Pötschke et al. 2010; Scaffaro et al. 2012), thermal stability (Hooshmand et al. 2011; John et al. 2013) and crystallinity (Mazinani et al. 2010) as well as mechanical properties (Haggenmueller et al. 2000; Yoon et al. 2004; Pötschke et al. 2005; Fornes et al. 2006; Mazinani et al. 2010; Scaffaro et al. 2012). For instance Scaffaro et al. (2012) prepared melt spun polyamide nanocomposite fibers using CNT as reinforcement. In this study plasma functionalized CNT were batch mixed with the polymer and melt spun to fibers. The composite fibers showed improved stiffness and tensile strength of approximately 200 and 30 % respectively, with the addition of 2 wt% CNT. In another study by Yoon et al. (2004) melt spun nylon/clay nanocomposite fibers with 5 wt% layered-silicates showed an improved modulus of approximately 30 % but decreased tensile strength by 25 %. CNC were used for first time as an additive for melt spun PLA fibers in a study by (John et al. 2013 and no improvements of the mechanical properties were obtained. The authors suggested that this was due to poor dispersion of the CNC in the PLA matrix. Later, our study on the comparison of different dispersion techniques of CNC in cellulose acetate butyrate (CAB) fibers, showed more promising results and a slight improvement of 17 % for the stiffness was observed (Hooshmand et al. 2014).

The key elements to improve the mechanical properties are the properties of the reinforcing phase, its size and the dispersion as well as its interaction with the matrix polymer. CNC have a modulus of approximately 138 GPa (Sakurada et al. 1962), high aspect ratio and large surface area and therefore have attracted attention as reinforcements in nanocomposites (Azizi Samir et al. 2005). In addition the hydroxyl groups on the CNC surface have a strong tendency for self-association (Van den Berg et al. 2007), which is advantageous for the formation of percolating architectures within the host polymer matrix (Capadona et al. 2009). These percolating architectures facilitate the stress transfer in the crystals network due to the presence of hydrogen bonding between the CNC (Capadona et al. 2008). However, the CNC–CNC interactions can also lead to aggregation during nanocomposite fabrication (particularly in non-polar matrices) and consequently a reduction in the mechanical properties of the materials compared to the predicted properties (Schroers et al. 2004; Capadona et al. 2007; Petersson et al. 2009). This emphasizes the importance of good dispersion in achieving improved mechanical properties. In our recent study (Hooshmand et al. 2014), we showed the potential of a sol–gel pre-process prior the to melt spinning of CAB nanocomposite fibers in order to improve the dispersion of the nanocrystals. This dispersion process was done avoiding the use of surfactants or surface modifications, because these treatments can lead to a poor interphase and thus suppress the reinforcing effect of the nanocrystals (Grunert and Winter 2002; Bondeson and Oksman 2007).

In this current study, the effect of increasing the weight fraction of CNC from 2 wt% to 10 wt% in CAB-based fibers manufactured using the process established earlier (Hooshmand et al. 2014) was investigated. The effect of the increased concentration on the mechanical and thermal performance of the fibers was evaluated as well as the effect of drawing these fibers. However, unlike the previous study, to decrease the residence time and consequently avoiding the thermal degradation of materials, the spinning process was carried out in continuous mode instead of batch mode. The influences of the fiber drawing and the CNC concentration on characteristics of the fibers were examined by X-ray diffraction, thermogravimetric analysis, dynamic mechanical thermal analysis and scanning electron microscopy. The mechanical properties of the fibers were evaluated using tensile testing and the results were compared to theoretical predictions using a micromechanical model commonly used for short-fiber composites.

Experimental

Materials

Cellulose acetate butyrate, supplied by Eastman Chemical Company (Kingsport, USA) with butyrate content of 46 wt%, acetyl content of 2 wt% and hydroxyl content of 4.8 wt% was used as the matrix polymer. CAB is a thermoplastic and it is produced through the esterification of cellulose and can be used

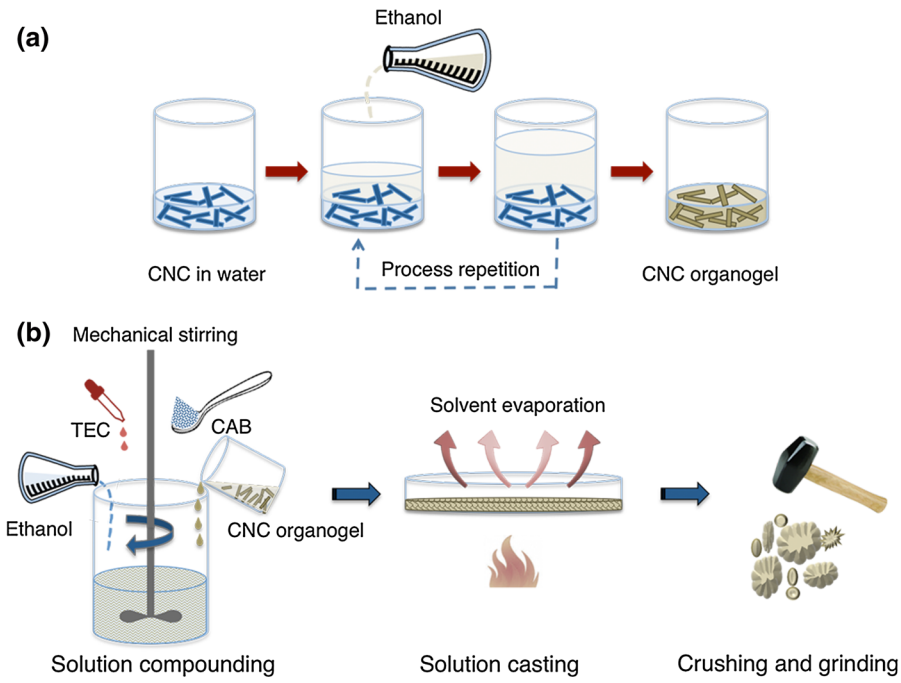

Fig. 1 **a** Schematic view of solvent exchange process using sol–gel technique. **b** Nanocomposite preparation by solution mixing

as substitute for petroleum-based plastics (Park et al. 2004). The main drawback of cellulose ester is that its melt temperature is above its decomposition temperature and also that it is very brittle. To overcome these problems a plasticizer has to be used.

Triethyl citrate (TEC) $C_{12}H_{20}O_7$ supplied by Fluka Chemie GmbH (Buchs, Switzerland) is an ester of citric acid and was used as plasticizer.

Sulfuric acid (96 %) for acid hydrolysis as well as ethanol absolute (99.99 %) for the preparation of CNC organo-gel and to dissolve CAB were purchased from VWR.

Never-dried dissolving cellulose residue (sludge) provided by Domsjö Fabriker AB (Örnsköldsvik, Sweden) was used as raw material for the preparation of the CNC. CNC were extracted by acid hydrolysis based on the method reported earlier (Herrera et al. 2012).

Preparation of cellulose nanocomposite

CNC and ethanol organo-gels were prepared following the procedure described by Siqueira et al. (2011) whereby a suspension of 8.0 mg/ml of CNC in a beaker was subjected to a brief sonication to homogenize it and remove air bubbles. Then 350 ml ethanol was gently added on top of the CNC suspension. This organic layer on the top of the aqueous dispersion was slightly agitated and exchanged once a day to accelerate the solvent exchange. The gel-like CNC ethanol organo-gel was formed after 6–7 days and then broken using bath sonication (Fig. 1a).

Watson et al. (2013) studied the influence of different organic liquids on the nanostructure of precipitated phosphoric acid swollen cellulose. They suggested that the gel-like material formed by washing cellulose with ethanol could be due to the formation of interchain hydrogen bonds that potentially inhibit the formation of intrachain hydrogen bonds. Probably similar mechanism happens during the sol–gel process used in this study.

The process of mixing was similar to the one described by Siqueira et al. (2011) and Hooshmand et al. (2014). First, the CAB was dissolved in ethanol to form 15 wt% solution using mechanical stirring for 12 h at room temperature. The dissolved CAB was then mixed with TEC (15 % weight fraction of the final nanocomposite). The organo-gels of CNC (2 and 10 wt%) were added to the CAB–TEC mixture. The CAB–TEC–CNC suspensions were mixed using magnetic stirring for 4 h followed by ultrasonication for 3 min to get good dispersion of CNC in the mixture. The suspensions were then casted in polystyrene Petri dishes and left in a vacuum oven at 60 °C for 24 h. For

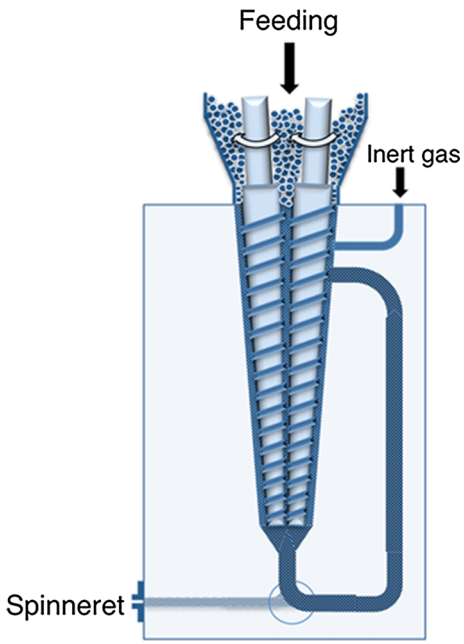

Fig. 2 Schematic view of the twin-screw micro-compounder in continuous mode (DSM Xplore, Geleen, The Netherland)

the first 5 h, a pressure of 800 mbar was used before a full vacuum was applied, to avoid bubble formation. The films were removed from the Petri dishes using deionized water and left in an oven at 60 °C overnight and then were crushed and pulverized using a Warring blender and dried in an oven for one week (60 °C at atmospheric pressure) to remove any remaining solvent. The same procedure was applied to prepare unreinforced CAB–TEC (85–15 wt%) as a reference material. Figure. 1b shows the schematic of the nanocomposite preparation.

Melt spinning and fiber drawing

All three materials (CAB–TEC, CAB–TEC–2CNC and CAB–TEC–10CNC) were melt spun by a 15 ml twin-screw micro-compounder, DSM Xplore (Geleen, The Netherlands) at 160 °C in an argon atmosphere. To decrease the residence time and consequently avoid thermal degradation of the materials, melt spinning was carried out in continuous mode (see Fig. 2). The feeding was done manually from top of the micro-compounder and a force control mode (4,000–5,000 N) was chosen instead of screw speed control to achieve more uniform fibers. A 0.4 mm spinneret was attached to the outlet of the micro-compounder to extrude the fiber monofilaments. The as-spun fibers were cooled by air and collected directly on a rotating take-up roll, which was placed 50 cm from spinneret. The as-spun fibers were then solid-state drawn with ratio of 1.5 over two godet-rolls (FOURNÉ Polymertechnik, Alfter, Germany see Fig. 3) in a separate process to the melt spinning. The first roll was heated to approximately 105 °C and the second one had a temperature of 90 °C. The compositions of the fibers produced are summarized in Table 1.

Analysis

Flow birefringence was investigated using two polarizing filters and a lamp to indicate the dispersion of the CNC in water as well as dispersion of the CNC organo-gel in the dissolved CAB–TEC suspension. Several authors consider the presence of flow birefringence as a preliminary indication of successful isolation and dispersion of the CNC in an organic solvent (Azizi Samir et al. 2004; Ayuk et al. 2009; Siqueira et al. 2009; Herrera et al. 2012).

To characterize the isolated CNC, a drop of a very diluted suspension of the isolated CNC in water was deposited on a mica surface and dried at room temperature. The atomic force microscopy (AFM) in tapping mode was performed on a Veeco Multimode Scanning Probe (Santa Barbara, CA, USA) with Nanoscope V software to collect the height and amplitude images.

A JEOL JSM-6460LV scanning electron microscope (SEM) with the acceleration voltage of 15 kV was used to study the morphology of the fibers. The fibers were sputter-coated with gold prior the analysis to avoid charging.

To study the crystallinity of the materials, X-ray diffraction was performed using a PANalytical Empyrean (Almelo, The Netherlands) with CuKα radiation (wave length of 1.5405 Å) with 2θ scan range of 5°–40°. For sample preparation, a bundle of fibers were placed between two metal plates and pressed for 1 min at 50 °C to make film, which was cut and placed in the sample holder to run the examination.

To determine the effect of residence time on thermal degradation of the material during the spinning process, the isothermal stability of crushed CAB–TEC and its nanocomposites were examined at 160 °C for 30 min on a TA instrument TGA-Q500 (New

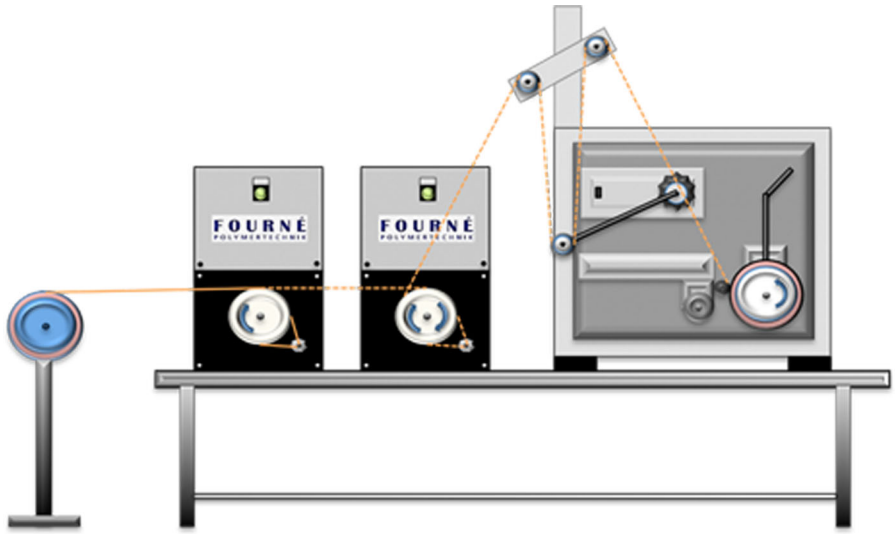

Fig. 3 Schematic view of the fiber drawing (FOURNE Polymertechnik, Alfter, Germany)

Table 1 The code, composition and draw ratio of the fibers

Sample	CAB (wt%)	CNC (wt%)	TEC (wt%)	Draw ratio
CAB–TEC_{AS}	85	0	15	0
CAB–TEC–2CNC_{AS}	83	2	15	0
CAB–TEC–10CNC_{AS}	75	10	15	0
CAB–TEC_{DR}	85	0	15	1.5
CAB–TEC–2CNC_{DR}	83	2	15	1.5
CAB–TEC–10CNC_{DR}	75	10	15	1.5

Castle, DE, USA) in a nitrogen atmosphere. In addition, thermal properties of the as-spun fibers were studied by the same instrument in ramp mode (20 °C/min from 30 to 600 °C).

Dynamic mechanical analysis of the spun fibers was performed on a TA instrument DMA-Q800 (New Castle, DE, USA) using in tensile mode and a fiber measurement tool with 15 mm gauge length. Prior to testing, fibers were placed in an oven for 1 h and 30 °C. The measurement was carried out at a constant frequency of 1 Hz, 0.1 % strain and a preload force of 0.01 N. The temperature range was 30–130 °C and a heating rate of 3 °C/min was used.

A universal testing machine, Shimadzu Autograph AG-X (Kyoto, Japan) equipped with a 100 N load cell was used to study the mechanical properties of the fibers. All the samples were placed in an oven for 1 h at 30 °C prior to testing. The tests were performed at room temperature using a constant speed of 5 mm/min and a preload of 0.1 N. The gauge length was 50 mm and the samples were mounted on paper frames before being tested. The fiber diameters of each fiber tested were measured using a Leitz Dialux optical microscope (Leica, Wetzlar, Germany). The average value and standard deviation of four replicates for each sample were calculated. In addition, statistical analysis based on the ANOVA and Tukey-HSD multiple comparison test at a 5 % significance level was used to test for significant differences. In this comparison, the values for the as-spun fibers were compared with one another and so were the values for the drawn fibers.

The reinforcing effect of CNC on polymers was modeled using a simple rule of mixtures based micromechanical model usually implemented for short-fiber composites (Andersons et al. 2006). Using this, the modulus, E, in the loading direction can be predicted based on the properties of the reinforcing elements and the matrix as

$$E = \eta_f \eta_o \mathrm{E}_f v_f + \left(1 - v_f\right) E_m \tag{1}$$

where

$$\eta_f = 1 - \frac{\tanh(\beta l/2)}{\beta l/2} \tag{2}$$

and

$$\beta = \frac{1}{r_f}\sqrt{\frac{2G_m}{E_f \ln\left(R/r_f\right)}} \tag{3}$$

and where E_f is the elastic modulus of the CNC, $E_m$is the elastic modulus of the matrix, v_f is the CNC volume fraction and $\eta_f$is the CNC length efficiency given by Eq. 2 and η_o is an orientation factor. In Eqs. 2 and 3, l is the length of the CNC, and assumed to be 240 nm (Siqueira et al. 2011), r_f is the fibers radius and set to the average value of 3.9 nm obtained from AFM. G_m is the shear modulus of the matrix and we assume that the matrix is isotropic and that $G_m = E_m/2(1 + v)$ with $v = 0.3$. $R/r_f$is the ratio of the interfiber distance to the CNC radius, which can be calculated from $\sqrt{K_R/v_f}$, where K_R is a packing number. For rectangular packing this is $\pi/4$, and is the number used here for these randomly orientated CNC (Andersons et al. 2006). In all cases E_f is assumed to be 138 GPa (Sakurada et al. 1962).

The theoretical value of E was calculated from Eqs. 1–3 for both fiber fractions of CNC with the volume fraction converted from the mass fraction under the assumption of no voids in the composite. In case of as-spun fibers, the crystals are assumed to be 3D randomly orientated, hence the orientation factor, η_o, was set to 0.2 (Andersons et al. 2006) and E_m set to the measured value of the modulus of the matrix-only fibers. In case of drawn fibers, E_m was set to the matrix-only drawn fiber's modulus and η_o was assumed to be 1 in the Eq. 1.

Results and discussion

Cellulose nanocrystals characterization

Figure 4a shows the flow birefringence of the cellulose nanocrystals in suspension. For comparison Fig. 4b is pure water. The pattern shown in Fig. 4a indicated a nematic liquid crystalline alignment, showing the existence of crystals after hydrolyzing. Figure 4c shows the flow birefringence of CNC organo-gel mixed with the CAB–TEC ethanol solution, confirming the dispersion and distribution of crystals. Again for comparison Fig. 4d is the CAB–TEC in absence of the CNC.

Figure 5 shows the structure and size of the prepared CNC analyzed by AFM. The height and amplitude show the presence of well-isolated and dispersed crystals in the nanometer scale with diameters in the range of 4–12 nm. To avoid the effects of broadening, only the height of crystals were measured and considered as the nanocrystals diameter.

Spinning and fiber drawing of nanocomposite fibers

Having well-dispersed nanoparticles in the matrix is very important for spinning of the nanocomposites fibers. Since the diameter of the fibers is small, even small aggregation of the nanoreinforcements can cause spin failure. In this study CAB–TEC as-spun nanocomposite fibers were successfully prepared using a two-step process involving (1) composite preparation using sol–gel process as the dispersion technique followed by solution casting, (2) continuous melt spinning. The produced fibers were uniform and had diameters in range of 340–450 μm. The variation between fiber diameters is most likely due to variation in the spinning rate. This is because the materials were fed manually and hence the amount of materials inside the compounder was changing during the process. To allow for this, force control mode was chosen instead of screw

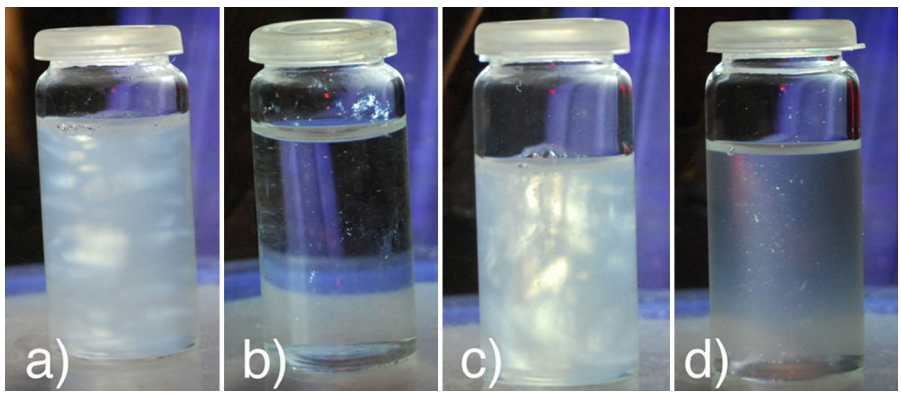

Fig. 4 Flow birefringence of **a** CNC in water, **b** water, **c** CAB–TEC–CNC and **d** CAB–TEC

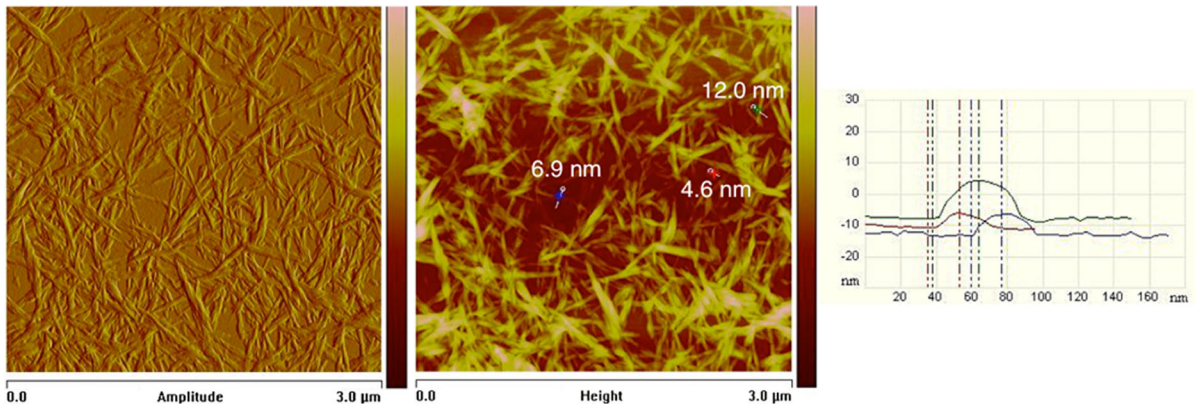

Fig. 5 AFM images of amplitude, height and crystals dimension measurement of the height image

speed control mode. However, although the fibers using this mode will be more uniform than using screw speed control some variation in the fibers diameter will still exist due to variation in the spinning rate.

The fibers were drawn successfully up to a drawing ratio of 1.5. The drawn fibers were also uniform and had diameters in range of 295–395 µm. The fiber drawability was highly sensitive to the addition of the CNC, which leads to lower elongation and thus causes breakage of the nanocomposite fibers (particularly 10 wt% CNC) under the drawing process. Hence, drawing at higher ratios than 1.5 (DR = 1.5) was not possible. Similar limitations of nanocomposite fiber drawability have been earlier reported by others (Solarski et al. 2008; Pötschke et al. 2010; John et al. 2013). It can be noted, however, from preliminary experiments on drawing CAB–TEC only fibers up to factor of 3, that no significant improvement could be observed after ratio of 1.5.

Microscopy

Figure 6 shows SEM micrograph of the surface of the as-spun and drawn CAB–TEC fibers and their nanocomposites containing 2 and 10 wt%. The micrographs indicated uniform diameters for all fibers and no defects such as microcracks or increased surface roughness were observed on the surfaces of the nanocomposite fibers. Similar results were reported by Hooshmand et al. (2014) for CAB–TEC nanocomposite fibers containing 2 wt% CNC using sol–gel process whereas an increase in surface roughness for PLA fibers reinforced with CNC was reported by John et al. (2013). Having no clusters or agglomerates on the surface of the fibers even for 10 wt% CNC indicates that CNC were well-dispersed in the matrix.

X-ray diffraction

The XRD analysis of the nanocomposite fibers was studied as a function of the CNC content, and the corresponding diffractograms are shown in Fig. 7. All of the CAB fibers exhibited a rather low crystalline structure with two peaks angle around $2\theta = 6°$ and 20°, which were assigned to crystalline segment of CAB (Rodríguez et al. 1998; Kosaka et al. 2006). The broad peak of CAB–TEC indicated highly amorphous CAB polymer. The XRD pattern of pure cellulose crystals displayed three well-defined diffraction peaks at 14.8, 16.4 and 22.6, exhibiting typical diffraction of cellulose I (Segal and Conrad 1957; Segal et al. 1959). The shoulder at 22.6° in both composites confirms the presence of CNC, however the two other peaks of CNC did not appear in the diffractograms. This is assumed to be because these peaks are small and the amount of the CNC (max. 10 %) is low.

Thermal properties

Figure 8a indicates the isothermal stability of the crushed CAB–TEC and its nanocomposites prior to spinning at 160 °C. It can be seen that after approximately 3 min, the materials start to be degraded. In addition, increasing the CNC content caused a slight increase in rate of degradation. For this reason, it was necessary to reduce the residence time as much as possible and the use of continuous mode allowed a substantial reduction in the residence time to be achieved.

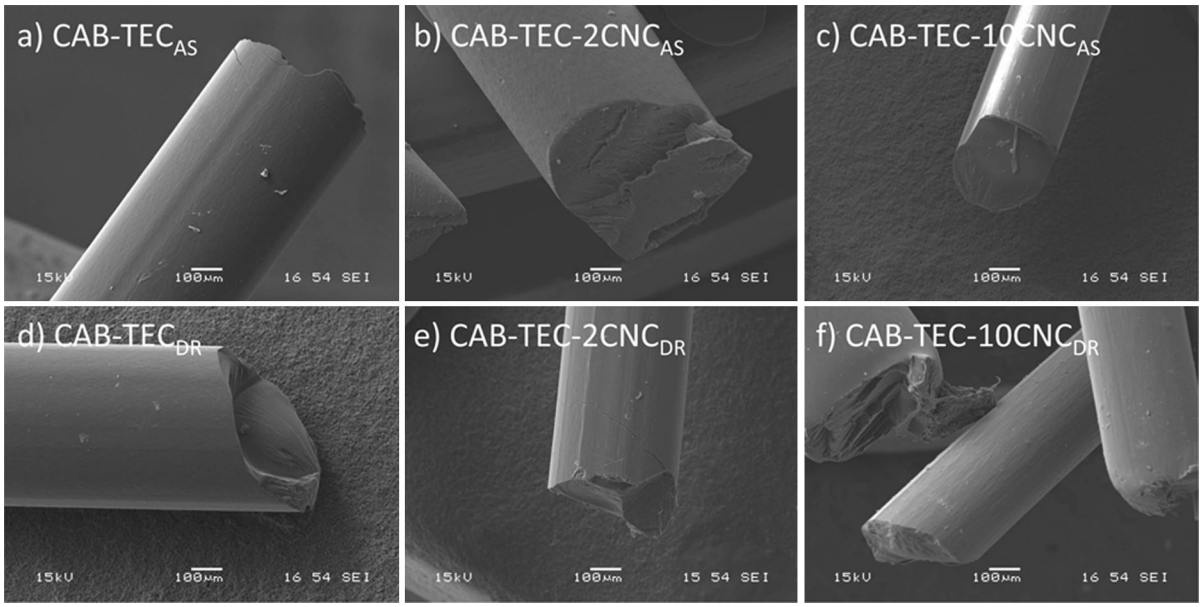

Fig. 6 SEM image of the both as-spun and drawn fibers. **a** CAB–TEC$_{AS}$, **b** CAB–TEC–2CNC$_{AS}$, **c** CAB–TEC–10CNC$_{AS}$, **d** CAB–TEC$_{DR}$, **e** CAB–TEC–2CNC$_{DR}$, and **f** CAB–TEC–10CNC$_{DR}$

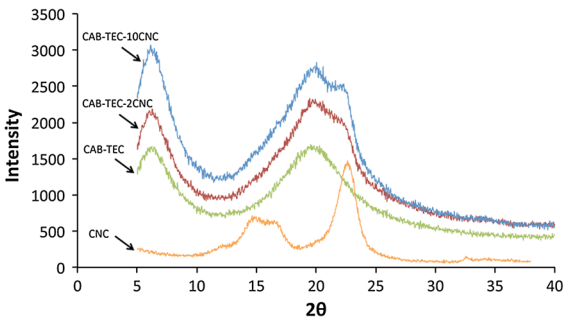

Fig. 7 XRD diffractograms of the pure CNC as well as CAB–TEC and its nanocomposite fibers

The TGA results of CAB–TEC and its nanocomposite as-spun fibers as well as prepared cellulose crystals are shown in Fig. 8b. As seen all produced fibers have thermal stability up to ≈300 °C, but the addition of CNC slightly decrease the thermal stability of the composites, because of the lower thermal stability of the CNC compared to the matrix.

Mechanical properties

The representative curves for the storage modulus (E′), loss modulus (E″) and tan δ of the CAB–TEC and its nanocomposite fibers as a function of temperature are shown in Fig. 9. In the case of the as-spun fibers, across the whole temperature range of the experiment, the nanocomposite fibers showed higher storage modulus compared to the CAB–TEC fibers. The materials showed glassy behavior until the transition around 80 °C and thereafter the storage modulus dropped rapidly. The storage modulus of the materials at 30 and 130 °C are given in Table 2 for comparison. At 30 °C, the CAB–TEC$_{AS}$ fiber exhibited a storage modulus (E′) of 908 MPa, and the addition of 2 % and 10 % CNC to the matrix, increased it by 47 and 149 %, respectively. A greater reinforcing effect were observed in the transition region at 130 °C, where the storage modulus increased from 5.4 to 12.3 MPa (≈130 %) and 85.4 MPa (≈1,500 %) for the 2 and 10 % CNC nanocomposites, respectively. The improvement in storage modulus for both nanocomposite fibers can be evidence for a good dispersion of the CNC in the matrix. Improvements in storage modulus for CAB by the addition of CNC have also been reported earlier, though direct comparison are difficult because of differences in concentrations of CNC and plasticizer (Bondeson et al. 2007; Ayuk et al. 2009; Siqueira et al. 2011).

The loss modulus curves shown in Fig 9a were analyzed to understand the effect of CNC on the relaxation peak temperature. These E″ curves shows a shoulder around 99 °C for CAB–TEC and

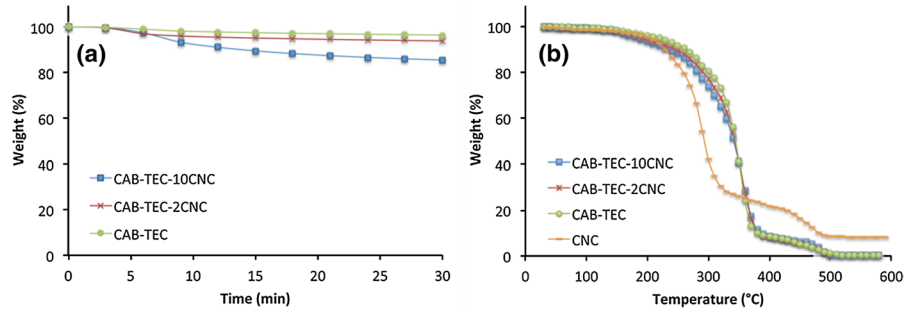

Fig. 8 **a** Isothermal stability of the crushed CAB–TEC and its nanocomposite prior to melt spinning. **b** Thermal stability of the CNC, CAB–TEC and its nanocomposite fibers

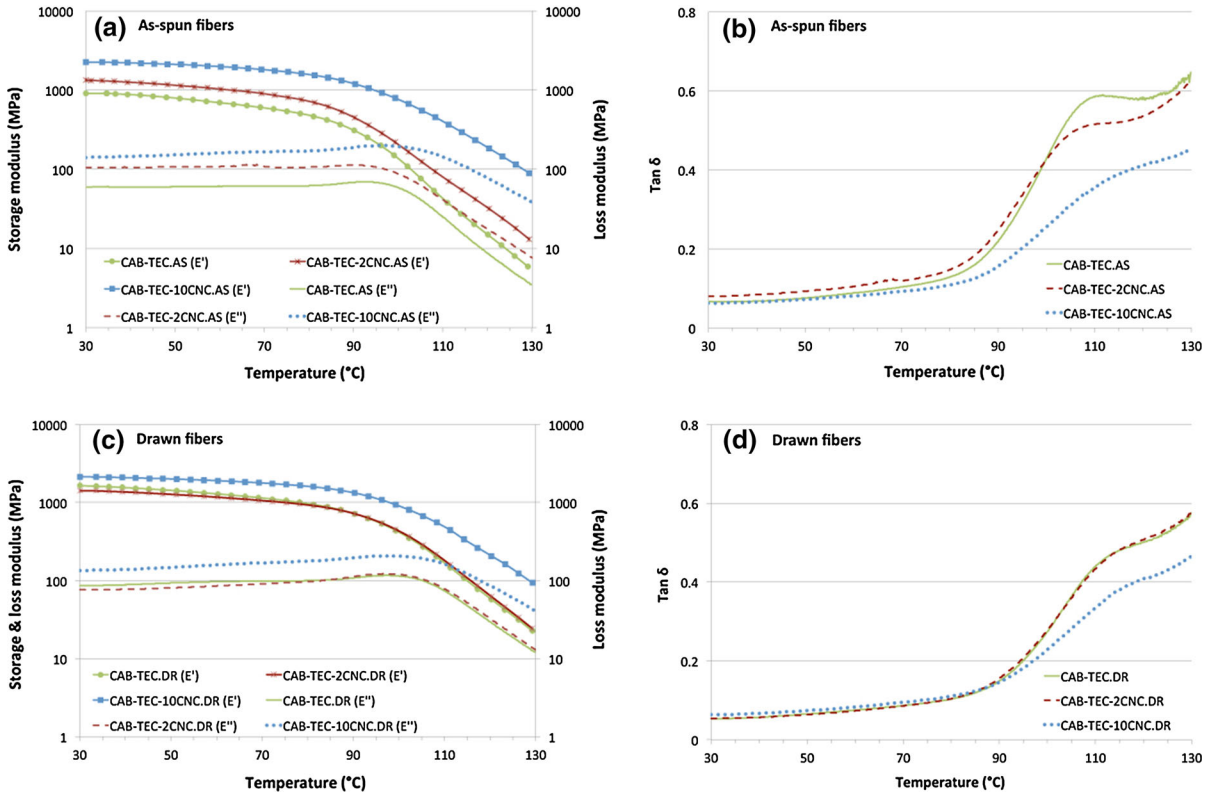

Fig. 9 Dynamic mechanical properties of prepared fibers, **a** storage and loss modulus, **b** tan delta of as-spun fibers and **c** storage and loss modulus, **d** tan delta of drawn fibers

nanocomposite with 2 % CNC. This shoulder was slightly shifted to 106 °C in the case of nanocomposites with 10 % CNC. This positive shift of 7 °C for CAB–TEC–10CNC$_{AS}$ indicates favorable interactions between CNC and CAB, which induce restriction of polymer chain mobility owing to good dispersion of CNC in CAB. The tan δ curves for the as-spun fibers, shown in Fig 9c, show no clear tan δ peak, but the shoulder around 110 °C may be attributed to the tan δ peak. Unfortunately, it was not possible to continue the experiment above 130 °C because of the form of the sample and the high amount of plasticizer used. This is because the single fiber is more prone to softening than the thin film and the plasticizer reduced the melt temperature making the temperature at which the tan δ peak occurs (the relaxation temperature) very close to the melt temperature. Similar results regarding tan δ are reported by Ayuk et al. (2009) and Siqueira et al. (2011) for samples where CNC were dispersed using solvent exchange techniques, however

Table 2 Storage modulus (E′) of the CAB–TEC and its nanocomposite fibers at 30 and 130 °C

Sample	Storage modulus (MPa)	
	At 30 °C	At 130 °C
CAB–TEC_{AS}	908	5.4
CAB–TEC–2CNC_{AS}	1,332	12.3
CAB–TEC–10CNC_{AS}	2,260	85.4
CAB–TEC_{DR}	1,641	21.1
CAB–TEC–2CNC_{DR}	1,422	22.4
CAB–TEC–10CNC_{DR}	2,133	88.0

Bondeson et al. (2007) reported a remarkable shift of 31 °C for the tan δ peak by using a liquid feeding method in extruder. In Fig. 9c it can also be seen that the intensity of the tan δ peak decreased with addition of CNC, which indicates lower amounts of amorphous regions taking part in the transition in the case of nanocomposites compared to the plasticized matrix.

Drawing of the fibers led to an improvement in storage modulus of the CAB–TEC fibers. As it can be seen in Fig. 9b that across the temperature range tested CAB–TEC_{DR} and CAB–TEC–2CNC_{DR} have very similar storage modulus, while CAB–TEC–10CNC_{DR} had a higher storage modulus. Table 2 shows that the storage modulus of CAB–TEC_{DR} fiber was increased by 80 and 290 % at 30 and 130 °C respectively compared to CAB–TEC_{AS} at the same temperatures. However, the difference in storage modulus of the as-spun and drawn nanocomposite fibers are negligible. The relaxation point, as shown by the shoulder of the loss modulus curves of CAB–TEC_{AS} and CAB–TEC_{DR} (Fig. 9a, b) shows a shift of 5 °C indicating that once drawn, a restriction of the polymer chain mobility is induced. As mentioned earlier, the addition of the CNC (in particular for 10 % CNC) restricted the mobility of the polymer chains as was seen from the positive shift of 7° in CAB–TEC–10CNC_{AS} fibers. Therefore, it is possible then this reduced mobility induced by the CNC restricts polymer alignment under drawing, and this would explain why drawing led to no improvement in storage modulus of the composite fibers compared to as-spun ones.

The results obtained from tensile test are summarized in Table 3 and the representative stress–strain curves are shown in Fig. 10. It can be seen that the low fraction of CNC (2 wt%) in the matrix had a great improvement on the modulus, increasing it by 57 % from 933 to 1,469 MPa. In addition, 2 wt% CNC had a slight improvement of 12 % (significant at the 5 % significance level) in the tensile strength. However a significant decreased in elongation of 66 % was also seen in the reinforced polymer, which shows that the CNC are restricting the movement of the polymer. The higher weight fraction of CNC (10 wt%) increased the tensile strength to 25.8 MPa and modulus to 1,770 MPa which is an increase of 23 % and 90 % respectively. Again, the elongation decreased, in this case by 73 %.

The dispersion technique used is thought to play an important role in reducing aggregation and hence obtaining these improved mechanical properties over that of the matrix alone. The support for this is from the fact that in some earlier studies, decreased mechanical properties of nano-reinforced fibers have been reported (Solarski et al. 2007,2008; John et al. 2013).

By comparing the obtained results with the study of Siqueira et al. (2011), who used a similar dispersion technique, it can be seen that the current study shows better improvement in stiffness particularly for the lower 2 % CNC concentration, however improvement in tensile strength was lower than the results reported by Siqueira et al. (2011). The result for the nanocomposite fiber produced here do not however match the improvements in CAB shown by Bondeson et al. (2007), where increases of 100 and 300 % for tensile strength and modulus were reported for CAB–15 %TEC–5 %CNC film produced by extrusion and compression molding with the CNC were fed as a suspension into an extruder.

In case of drawn fibers, stretching the fibers resulted in an improvement of 45 % for the strength and 59 % for the modulus for CAB–TEC_{DR} compared to as-spun ones. However, lower improvements were seen for the CAB–TEC–2CNC_{DR} and CAB–TEC–10CNC_{DR} fibers. In these fibers the strength increased by 10 % and 16 % and for the modulus by 2 % and 23 % compared to the as-spun fibers with the same CNC concentrations. Higher mechanical properties of CAB–TEC_{DR} are clearly the effect of the alignment of polymer chains in the direction of the applied load. Table 3 shows that CAB–TEC_{DR} and CAB–TEC–2CNC_{DR} have very similar stiffness, which is very close to the stiffness of the CAB–TEC–2CNC_{AS}. It seems that the reinforcing effect of the 2 % CNC in drawn fiber was negligible possibly because of the

Table 3 Fiber diameter, tensile strength, Young's modulus and strain at break of CAB–TEC and its nanocomposite fibers

Sample	Diameter (μm)	Tensile strength (MPa)	Young's modulus (MPa)	Strain (%)
CAB–TEC$_{AS}$	470 ± 15	20.9^{a} ± 0.9	933.4^{a} ± 9.4	21.2^{a} ± 3.1
CAB–TEC–2CNC$_{AS}$	393 ± 23	23.6^{b} ± 1.1	1,469.3^{b} ± 46.5	7.1^{b} ± 2.2
CAB–TEC–10CNC$_{AS}$	370 ± 13	25.8^{c} ± 0.3	1,770.2^{c} ± 30.1	5.7^{b} ± 1.5
CAB–TEC$_{DR}$	362 ± 21	30.5^{A} ± 3.0	1,483.4^{A} ± 46.5	4.1^{A} ± 0.4
CAB–TEC–2CNC$_{DR}$	396 ± 11	26.0^{A} ± 1.2	1,497.6^{A} ± 47.2	3.2^{B} ± 0.3
CAB–TEC–10CNC$_{DR}$	340 ± 36	29.9^{A} ± 3.7	2,184.9^{B} ± 135.4	2.3^{C} ± 0.5

Average values with same superscript letter in the same column are not significantly different at 5 % significance level based on ANOVA and Tukey−HSD multiple comparison test. The values for the as-spun fibers samples were compared with one another and so were the values for the drawn fibers samples

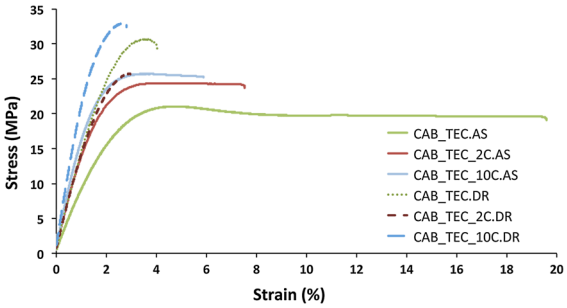

Fig. 10 Representative stress–strain curves of the CAB–TEC and its nanocomposite fibers

restriction of the alignment of the polymer chains due to the presence of the CNC, as mentioned earlier. But increasing the CNC concentration to 10 %, the stiffness was improved by 23 % compared to the reinforced as-spun fiber (CAB–TEC–10CNC$_{AS}$) indicating an alignment effect most likely from a combination of the alignment of both CNC and polymer chains.

The parameter values used in the short-fiber model described by Eqs. 1–3 to calculate theoretical values of the length efficiency, η_f, and modulus, E, of nanocomposite fibers are summarized in Table 4. In addition, to see how the improvements compare to what can be expected from these nanocomposites, both theoretical and measured values are shown in Fig. 11. As it can be seen for as-spun fibers, the measured value for CAB–TEC–2CNC$_{AS}$ was even greater than that the predicted by the model, which only predict an increase of 19 % (1,109 MPa). It seems therefore that the model does not completely capture the behavior of the composite. This is possibly

Table 4 Parameters used in the short-fiber model, described by Eqs. 1–3, to calculate theoretical values of the length efficiency (η_f) and modulus (E) of nanocomposite fibers

Parameter	CAB–TEC–2CNC$_{AS}$	CAB–TEC–10CNC$_{AS}$	CAB–TEC–2CNC$_{DR}$	CAB–TEC–10CNC$_{DR}$
E_f (MPa)	138,000	138,000	138,000	138,000
E_m (MPa)	933	933	1,483	1,483
G_m (MPa)	358^{a}	358^{a}	570^{a}	570^{a}
V_f (%)	1.64	8.35	1.64	8.35
R/r_f	6.92	3.07	6.92	3.07
r_f (nm)	3.9	3.9	3.9	3.9
l (nm)	240	240	240	240
β (x1e^{6})	13.29	17.46	16.76	22.02
η_o	0.2	0.2	1	1
η_f	0.42^{a}	0.54^{a}	0.52^{a}	0.63^{a}
E (MPa)	1,109^{a}	2,093^{a}	2,636^{a}	8,566^{a}

^{a} Calculated values from Eqs. 1–3

due to the fact that the model does not take into account the large surface area of the nanosized crystals that appears to lead to properties beyond that of a simple combination of those of the matrix and crystals. Note that this large surface area effect would only have a positive effect if there is a good interaction between the nanocrystals and the matrix. However, in the case of the higher concentration of CNC (10 wt%) the model predicted a more dramatic increase in the stiffness (124 %). The lower measured value compared to the theoretical one is thought to be due to some inhomogeneities. This means the crystal size is not exactly that which is assumed in the model. It is also possible that the surface area effect shown in the

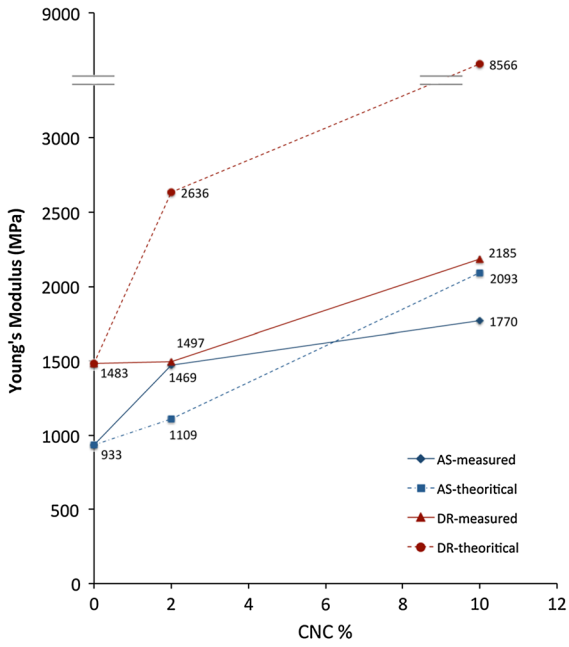

Fig. 11 Theoretical and experimental values of fibers stiffness for comparison

CAB–TEC–2CNC$_{AS}$ fiber still exists but is masked by effects of aggregation. It should be mentioned that this model strongly depends on the geometry of the fibers and any changes in length and diameter of the crystals can have a dramatic effect on the predicted values.

In case of drawn fibers, for CAB–TEC–2CNC$_{DR}$, the measured value is 57 % of the theoretical value, while by increasing the concentration of CNC to 10 wt%, the measured value is only 26 % of the predicted one. These lower values compared to the predicted ones, can indicate that there was no or very small orientation for CNC in the matrix.

Conclusion

In this study the effect of increased CNC concentration as well as the influence of fiber drawing on the melt spun CAB nanocomposite fibers were evaluated. Results showed that the combination of the used dispersion technique and melt spinning is a suitable technique to prepare nanocomposite fibers with higher concentrations of CNC (10 wt%). This is shown from the SEM microstructure study of the fibers, which indicated a defect-free smooth surface for both as-spun and drawn fibers.

The viscoelastic behavior of the fibers were studied and the results showed that addition of CNC increased the storage modulus of the fibers, the shift of relaxation temperature indicates good interaction between the CNC and the CAB and that the CNC increased the thermal stability.

The mechanical performance of the fibers showed that a 2 wt% CNC concentration increased the mechanical properties. This increase is above the predicted value from the micromechanical modeling and is possibly because of the large surface area and molecular interaction, which are not included in the fiber matrix models, and leads to properties beyond that of a simple combination of the matrix and the crystals. In the case of 10 wt% CNC concentration, both the tensile strength (23 %) and modulus (90 %) were improved, however the model predicted a higher stiffness than that was seen in the nanocomposites. This suggests some aggregation of the CNC in the matrix as the CNC concentration increases.

Fiber drawing was shown to have a positive effect on the mechanical properties of the 10 % CNC nanocomposites fibers. However, according to theoretical estimation, high orientation of the CNC should results in much higher properties. Hence the achieved improvement is thought to be due to only a slight orientation of both the matrix and CNC. However, the combined effect of reinforcing using CNC and drawing still provides even further improvement in mechanical properties.

Acknowledgments The authors gratefully acknowledge the Bio4Energy and VINNOVA for the financial support of this work as well as Domsjö Fabriker AB for the supplied materials.

References

Andersons J, Spārniņš E, Joffe R (2006) Stiffness and strength of flax fiber/polymer matrix composites. Polym Compos 27:221–229. doi:10.1002/pc.20184

Ayuk JE, Mathew AP, Oksman K (2009) The effect of plasticizer and cellulose nanowhisker content on the dispersion and properties of cellulose acetate butyrate nanocomposites. J Appl Polym Sci 114:2723–2730. doi:10.1002/app.30583

Azizi Samir MAS, Alloin F, Sanchez J, El Kissi N, Dufresne A (2004) Preparation of cellulose whiskers reinforced nanocomposites from an organic medium suspension. Macromolecules 37:1386–1393. doi:10.1021/ma030532a

Azizi Samir MAS, Alloin F, Dufresne A (2005) Review of recent research into cellulosic whiskers, their properties

and their application in nanocomposite field. Biomacromolecules 6:612–626. doi:10.1021/bm0493685

Bondeson D, Oksman K (2007) Dispersion and characteristics of surfactant modified cellulose whiskers nanocomposites. Compos Interfaces 14:617–630. doi:10.1163/156855407782106519

Bondeson D, Syre P, Oksman Niska K (2007) All cellulose nanocomposites produced by extrusion. J Biobased Mater Bioenergy 1:367–371. doi:10.1166/jbmb.2007.011

Capadona JR, Van Den Berg O, Capadona LA, Schroeter M, Rowan SJ, Tyler DJ, Weder C (2007) A versatile approach for the processing of polymer nanocomposites with self-assembled nanofibre templates. Nat Nanotechnol 2:765–769. doi:10.1038/nnano.2007.379

Capadona JR, Shanmuganathan K, Tyler DJ, Rowan SJ, Weder C (2008) Stimuli-responsive polymer nanocomposites inspired by the sea cucumber dermis. Science 319:1370–1374. doi:10.1126/science.1153307

Capadona JR, Shanmuganathan K, Trittschuh S, Seidel S, Rowan SJ, Weder C (2009) Polymer nanocomposites with nanowhiskers isolated from microcrystalline cellulose. Biomacromolecules 10:712–716. doi:10.1021/bm8010903

Fornes TD, Baur JW, Sabba Y, Thomas EL (2006) Morphology and properties of melt-spun polycarbonate fibers containing single- and multi-wall carbon nanotubes. Polymer 47:1704–1714. doi:10.1016/j.polymer.2006.01.003

Grunert M, Winter W (2002) Nanocomposites of cellulose acetate butyrate reinforced with cellulose nanocrystals. J Polym Environ 10:27–30. doi:10.1023/A:1021065905986

Haggenmueller R, Gommans HH, Rinzler AG, Fischer JE, Winey KI (2000) Aligned single-wall carbon nanotubes in composites by melt processing methods. Chem Phys Lett 330:219–225. doi:10.1016/S0009-2614(00)01013-7

Herrera MA, Mathew AP, Oksman K (2012) Characterization of cellulose nanowhiskers: a comparison of two industrial bio-residues. IOP Conference Series: Mat Sci Eng 31:012006. doi:10.1088/1757-899X/31/1/012006

Hooshmand S, Soroudi A, Skrifvars M (2011) Electro-conductive composite fibers by melt spinning of polypropylene/polyamide/carbon nanotubes. Synth Met 161:1731–1737. doi:10.1016/j.synthmet.2011.06.014

Hooshmand S, Cho S, Skrifvars M, Mathew AP, Oksman K (2014) Melt spun cellulose nanocomposite fibres: comparison of two dispersion techniques. Plast Rubber Compos 43:15–24. doi:10.1179/1743289813Y.0000000066

John MJ, Anandjiwala R, Oksman K, Mathew AP (2013) Melt-spun polylactic acid fibers: effect of cellulose nanowhiskers on processing and properties. J Appl Polym Sci 127:274–281. doi:10.1002/app.37884

Kosaka PM, Kawano Y, Fantini MC, Petri DF (2006) Structure and properties of maleated linear low-density polyethylene and cellulose acetate butyrate blends. Macromol Mater Eng 291:531–539. doi:10.1002/mame.200500413

Lee SH, Youn JR (2008) Properties of polypropylene/layered-silicate nanocomposites and melt-spun fibers. J Appl Polym Sci 109:1221–1231. doi:10.1002/app.28222

Mazinani S, Ajji A, Dubois C (2010) Structure and properties of melt-spun PET/MWCNT nanocomposite fibers. Polym Eng Sci 50:1956–1968. doi:10.1002/pen.21727

O'Brien JP, Aneja AP (1999) Fibres for the next millennium. Rev Prog Coloration 29:1–7. doi:10.1111/j.1478-4408.1999.tb00122.x

Park H, Misra M, Drzal LT, Mohanty AK (2004) "Green" nanocomposites from cellulose acetate bioplastic and clay: effect of eco-friendly triethyl citrate plasticizer. Biomacromolecules 5:2281–2288. doi:10.1021/bm049690f

Petersson L, Mathew AP, Oksman K (2009) Dispersion and properties of cellulose nanowhiskers and layered silicates in cellulose acetate butyrate nanocomposites. J Appl Polym Sci 112:2001–2009. doi:10.1002/app.29661

Pötschke P, Brünig H, Janke A, Fischer D, Jehnichen D (2005) Orientation of multiwalled carbon nanotubes in composites with polycarbonate by melt spinning. Polymer 46:10355–10363. doi:10.1016/j.polymer.2005.07.106

Pötschke P, Andres T, Villmow T, Pegel S, Brünig H, Kobashi K, Fischer D, Häussler L (2010) Liquid sensing properties of fibres prepared by melt spinning from poly(lactic acid) containing multi-walled carbon nanotubes. Compos Sci Technol 70:343–349. doi:10.1016/j.compscitech.2009.11.005

Rodríguez M, Vila-Jato JL, Torres D (1998) Design of a new multiparticulate system for potential site-specific and controlled drug delivery to the colonic region. J Control Release 55:67–77. doi:10.1016/S0168-3659(98)00029-7

Sakurada I, Nukushina Y, Ito T (1962) Experimental determination of the elastic modulus of crystalline regions in oriented polymers. J Polym Sci 57:651–660. doi:10.1002/pol.1962.1205716551

Scaffaro R, Maio A, Tito AC (2012) High performance PA6/CNTs nanohybrid fibers prepared in the melt. Compos Sci Technol 72:1918–1923. doi:10.1016/j.compscitech.2012.08.010

Schadler LS (2004) Polymer-based and polymer-filled nanocomposites. 77–153. doi:10.1002/3527602127.ch2

Schroers M, Kokil A, Weder C (2004) Solid polymer electrolytes based on nanocomposites of ethylene oxide-epichlorohydrin copolymers and cellulose whiskers. J Appl Polym Sci 93:2883–2888. doi:10.1002/app.20870

Segal L, Conrad C (1957) Characterization of cellulose derivatives by means of the X-ray diffractometer. Am Dyest Rep 46:637–642

Segal L, Creely J, Martin A, Conrad C (1959) An empirical method for estimating the degree of crystallinity of native cellulose using the X-ray diffractometer. Text Res J 29:786–794

Siqueira G, Bras J, Dufresne A (2009) Cellulose whiskers versus microfibrils: influence of the nature of the nanoparticle and its surface functionalization on the thermal and mechanical properties of nanocomposites. Biomacromolecules 10:425–432. doi:10.1021/bm801193d

Siqueira G, Mathew AP, Oksman K (2011) Processing of cellulose nanowhiskers/cellulose acetate butyrate nanocomposites using sol–gel process to facilitate dispersion. Compos Sci Technol 71:1886–1892. doi:10.1016/j.compscitech.2011.09.002

Solarski S, Mahjoubi F, Ferreira M, Devaux E, Bachelet P, Bourbigot S, Delobel R, Coszach P, Murariu M, silva Ferreira A, Alexandre M, Degee P, Dubois P (2007) (Plasticized) polylactide/clay nanocomposite textile: thermal,

mechanical, shrinkage and fire properties. J Mater Sci 42:5105–5117. doi:10.1007/s10853-006-0911-0

Solarski S, Ferreira M, Devaux E, Fontaine G, Bachelet P, Bourbigot S, Delobel R, Coszach P, Murariu M, Da Ferreira Silva A, Alexandre M, Degee P, Dubois P (2008) Designing polylactide/clay nanocomposites for textile applications: effect of processing conditions, spinning, and characterization. J Appl Polym Sci 109:841–851. doi:10.1002/app.28138

Van den Berg O, Schroeter M, Capadona JR, Weder C (2007) Nanocomposites based on cellulose whiskers and (semi) conducting conjugated polymers. J Mater Chem 17: 2746–2753. doi:10.1039/B700878C

Watson BJ, Hammouda B, Briber RM, Hutcheson SW (2013) Influence of organic liquids on the nanostructure of precipitated cellulose. J Appl Polym Sci 127:2620–2627. doi:10.1002/app.37540

Yoon K, Polk MB, Min BG, Schiraldi DA (2004) Structure and property study of nylon-6/clay nanocomposite fiber. Polym Int 53:2072–2078. doi:10.1002/pi.1630